SciencePG
Science Publishing Group

Thermodynamic Properties of Bcc Crystals Studied on Their High-Order Expanded Debye-Waller Factors and XAFS Application to Ferrite Iron

Dinh Quoc Vuong[1], Nguyen Van Hung[2]

[1]Quang Ninh Education & Training Department, Nguyen Van Cu, Ha Long, Quang Ninh, Vietnam

[2]Department of Physics, Hanoi University of Science, 334 Nguyen Trai, Thanh Xuan, Hanoi, Vietnam

Email address:
dinhquocvuongqn@gmail.com (D. Q. Vuong), hungnv@vnu.edu.vn (N. V. Hung)

Abstract: Thermodynamic properties of bcc crystals have been studied based on the anharmonic correlated Debye model high-order expanded Debye-Waller factors and X-ray absorption fine structure (XAFS). The many-body effects are taken into account in the present one-dimensional model based on the anharmonic effective potential that includes interactions of absorber and backscatterer atoms with their first shell near neighbors, where Morse potential is assumed to describe the single-pair atomic interaction. Analytical expressions for dispersion relation, correlated Debye frequency and temperature and four first temperature-dependent XAFS cumulants of bcc crystals have been derived using the many-body perturbation approach. The obtained cumulants are applied to calculating XAFS spectra and their Fourier transform magnitude. Numerical results for Fe, a ferrite crystal, are found to be in good agreement with experiment.

Keywords: Debye-Waller Factor, Effective Potential, Correlated Debye Model, XAFS, Iron

1. Introduction

X-ray Absorption Fine Structure (XAFS) has developed into a powerful technique for providing information on local atomic structure and thermal effects of the substances. The formalism for including anharmonic effects in XAFS is often based on the cumulant expansion approach [1] from which the expression for anharmonic XAFS has resulted as

$$\chi(k) = F(k) \frac{e^{-2R/\lambda(k)}}{kR^2} \text{Im} \left\{ e^{i\Phi(k)} \exp \left[2ikR + \sum_n \frac{(2ik)^n}{n!} \sigma^{(n)} \right] \right\}, (1)$$

where F(k) is the real atomic backscattering amplitude, k and λ are the wave number and mean free path of the photoelectron, respectively, Φ is net phase shift, $R = \langle r \rangle$ with *r* as the instantaneous bond length between absorber and backscatterer atoms, and $\sigma^{(n)}$ (n = 1, 2, 3, 4, …) are the cumulants describing the high-order expanded Debye-Waller

factors (DWFs).

Hence, the cumulants are very important for the accurate structural determinations (e.g., the coordination numbers and the atomic distances) from XAFS experiment, where the even cumulants contribute to the amplitude, the odd one to the phase of XAFS and for small anharmonicities, it is sufficient to keep the third and fourth cumulant terms [2]. If limiting to the fourth cumulant, the temperature T- and wave number k-dependent anharmonic contributions to the amplitude $F_A(k, T)$ and to the phase $\Phi_A(k, T)$ of XAFS are given by

$$F_A(k,T) = \exp \left(-\frac{2}{3} k^4 \sigma^{(4)}(T) \right),$$

$$\Phi_A(k,T) = -\frac{4k\sigma^2(T)}{R} \left(1 + \frac{R}{\lambda} \right) - \frac{4}{3} k^3 \sigma^{(3)}(T)$$, (2)

Many efforts have been made to develop procedures for the calculation and analysis of XAFS cumulants using the classical [3-5] and quantum [6-16] theories. Unfortunately, there is still few methods for studying XAFS DWFs with high-order expansion and no theoretical result on XAFS of bcc crystals while their experimental results are available [17].

The purpose of this work is to study the thermodynamic properties of bcc crystals based on temperature dependence of their high-order expanded DWFs in the anharmonic correlated Debye model (ACDM) [16] and XAFS Fourier transform magnitude. The derivation is presented in Section 2 for the analytical expressions of four first temperature-dependent XAFS cumulant of bcc crystals using the many-body perturbation approach (MBPA) [18], the dispersion relation and anharmonic effective potential parameters, where Morse potential is assumed to describe the single-pair atomic interaction. The obtained cumulants are applied to calculating XAFS spectra and their Fourier transform magnitudes (FTM). Numerical results for Fe, a ferrite crystal, (Section 3) are compared to experiment [17] which show good agreement. The conclusions of the obtained results are presented in Sect. 4.

2. Formalism

In order to include the anharmonic effects, Hamiltonian of the system is written in the summation of the harmonic and anharmonic components, H_0 and H_a, respectively

$$H = H_0 + H_a , \quad H_a = H_c + H_q , \quad (3)$$

where the anharmonic component H_a contain the cubic H_c and quartic H_q terms including the anharmonic interatomic effective potential parameters of bcc crystals.

The anharmonic interatomic *effective potential* expanded up to the fourth order in the present theory for bcc crystals can be expressed as a function of the displacement $x = r - r_0$ along the bond direction with r and r_0 being the instantaneous and equilibrium distances between absorber and backscatterer atoms, respectively

$$V_{eff}(x) \approx \frac{1}{2} k_{eff} x^2 + k_{3eff} x^3 + k_{4eff} x^4 , \quad (4)$$

where k_{eff} is the effective local force constant, k_{3eff} and k_{4eff} are the anharmonic parameters giving an asymmetry of the anharmonic effective potential.

For bcc crystals, each atom is bonded to 8 near neighbors. Then, the effective potential Eq. (4) defined based on the first shell near neighbor contribution approach (FSNNCA) has the form

$$V_{eff}(x) = V(x) + 2V\left(-\frac{x}{2}\right) + 6V\left(\frac{x}{6}\right) + 6V\left(-\frac{x}{6}\right), \quad (5)$$

which is the sum over not only the term V(x) describing the pair-interaction between absorber and backscatterer atoms but also the other terms describing the projections of their

pair-interactions with 14 first shell near neighbors of bcc crystals along the bond direction excluding the absorber and backscatterer themselves whose contributions are already described by V(x).

Applying Morse potential expanded up to the fourth order as

$$V(x) = D\left(e^{-2\alpha x} - 2e^{-\alpha x}\right) \approx D\left(-1 + \alpha^2 x^2 - \alpha^3 x^3 + \frac{7}{12}\alpha^4 x^4\right) \quad (6)$$

to each term of Eq. (5) and comparing the result to Eq. (4), we obtain the values of $k_{eff}, k_{3eff}, k_{4eff}$ for bcc crystals in terms of Morse potential parameters

$$k_{eff} = \frac{11}{3} D\alpha^2 , \quad k_{3eff} = -\frac{3}{4} D\alpha^3 , \quad k_{4eff} = \frac{1715}{2592} D\alpha^4 , \quad (7)$$

where α describes the width of the potential and D is dissociation energy.

Hence, the anharmonic effective potential for bcc crystals of Eq. (5) has resulted as

$$V_{eff}(x) \approx \frac{11}{6} D\alpha^2 x^2 - \frac{3}{4} D\alpha^3 x^3 + \frac{1715}{2592} D\alpha^4 x^4 . \quad (8)$$

Note that the above mentioned lattice contributions based on the FSNNCA, to the oscillation between absorber and backscatterer atoms described by the projections of their pair-interactions with 14 first shell near neighbors along the bond direction, make it possible to take into account the many-body effects in the present one-dimensional model for bcc crystals.

Derivation of the present ACDM for bcc crystals using the MBPA [18] is based on the dualism of an elementary particle in quantum theory, i.e., its corpuscular and wave property. Then, we can describe the system in Debye model involving all different frequencies up to the Debye frequency as a system consisting of many bodies, i.e., of many phonons, each of which corresponds to a wave having frequency ω(q) and wave number q varied in the first Brillouin zone (BZ).

For this purpose, the displacement u_n's in the parameter x in terms of the displacement of nth atom u_n of the one dimensional chain described by

$$x_n = u_{n+1} - u_n \quad (9)$$

is related to the phonon displacement operators A_q [19] in the form

$$u_n = \sqrt{\frac{\hbar}{2NM}} \sum_q \frac{e^{iqan}}{\sqrt{\omega(q)}} A_q , \quad A_q = A_{-q}^+ , \quad \left[A_q, A_{q'}\right] = 0 \quad (10)$$

to be given by

$$x_n = \sum_q e^{iqan} f(q) A_q , \quad f(q) = \sqrt{\frac{\hbar}{2NM\omega(q)}}\left(e^{iqa} - 1\right), \quad (11)$$

where N is atomic number, M is the mass of composite atoms and a is lattice constant.

The frequency $\omega(q)$ contained in Eqs. (10) and (11) and then in all cumulant expressions derived for the vibration between absorber and backscatterer atoms in XAFS process describes the dispersion relation. Using the local force constant of the first equation of Eqs. (7), it has resulted as

$$\omega(q) = 2\alpha\sqrt{\frac{11D}{3M}}\left|\sin\left(\frac{qa}{2}\right)\right|, \quad |q| \le \frac{\pi}{a}. \tag{12}$$

Using the above results in the MBPA [18], we have derived the analytical expressions for XAFS DWFs presented in terms of cumulant expansion up to the fourth order for bcc crystals.

The first cumulant describing the net thermal expansion or disorder in XAFS theory has resulted as

$$\sigma^{(1)}(T) = \langle x \rangle = \sigma_0^{(1)} \int_0^{\pi/a} \omega(q)\frac{1+Z(q)}{1-Z(q)}dq = \frac{\sigma_0^{(1)}}{\sigma_0^2}\sigma^2, \tag{13}$$

$$\sigma_0^{(1)} = \frac{81a\hbar}{484\pi D\alpha}, \quad Z(q) = \exp(\beta\hbar\omega(q)), \quad \beta = 1/k_BT.$$

Here, σ^2 is second cumulant describing the mean square relative displacement (MSRD) and has the following form

$$\sigma^2(T) = \langle x^2 \rangle = \sigma_0^2 \int_0^{\pi/a} \omega(q)\frac{1+z(q)}{1-z(q)}dq, \quad \sigma_0^2 = \frac{3\hbar a}{22\pi D\alpha^2}. \tag{14}$$

The third cumulant is the mean cubic relative displacement (MCRD) describing the asymmetry of the pair distribution function in XAFS theory and has resulted as

$$\sigma^{(3)}(T) \cong \langle x^3 \rangle - 3\langle x^2 \rangle\langle x \rangle = \sigma_0^{(3)} \int_0^{\pi/a} dq_1 \int_{-\pi/d}^{\pi/a-q_1} dq_2 \frac{\omega(q_1)\omega(q_2)\omega(q_1+q_2)}{\omega(q_1)+\omega(q_2)+\omega(q_1+q_2)}$$

$$\times\left\{1+6\frac{\omega(q_1)+\omega(q_2)}{\omega(q_1)+\omega(q_2)-\omega(q_1+q_2)}\frac{e^{\beta\hbar[\omega(q_1)+\omega(q_2)]}-e^{\beta\hbar\omega(q_1+q_2)}}{\left(e^{\beta\hbar\omega(q_1)}-1\right)\left(e^{\beta\hbar\omega(q_2)}-1\right)\left(e^{\beta\hbar\omega(q_1+q_2)}-1\right)}\right\}, \tag{15}$$

$$\sigma_0^{(3)} = \frac{114\times10^{-4}\hbar^2 a^2}{\pi^2 D^2\alpha^3}.$$

The fourth cumulant describes the anharmonic contribution to XAFS amplitude. It has been derived and given by

$$\sigma^{(4)}(T) \cong \langle x^4 \rangle - 3\langle x^2 \rangle^2 = \sigma_0^{(4)} \int_0^{\pi/a} dq_1 \int_0^{\pi/a-q_1} dq_2 \int_{-\pi/a}^{\pi/a-(q_1+q_2)} dq_3 \frac{\omega(q_1)\omega(q_2)\omega(q_3)\omega(q_4)}{\omega(q_1)+\omega(q_2)+\omega(q_3)+\omega(q_4)}$$

$$\times\left\{1+8\frac{Z(q_1)Z(q_2)Z(q_3)-Z(q_4)}{(Z(q_1)-1)(Z(q_2)-1)(Z(q_3)-1)(Z(q_4)-1)}\frac{\omega(q_1)+\omega(q_2)+\omega(q_3)}{\omega(q_1)+\omega(q_2)+\omega(q_3)-\omega(q_4)}\right.$$

$$\left.+6\frac{Z(q_1)Z(q_2)-Z(q_3)Z(q_4)}{(Z(q_1)-1)(Z(q_2)-1)(Z(q_3)-1)(Z(q_4)-1)}\frac{\omega(q_3)+\omega(q_4)}{\omega(q_1)+\omega(q_2)-\omega(q_3)-\omega(q_4)}\right\}, \tag{16}$$

$$\sigma_0^{(4)} = \frac{165\times10^{-4}\hbar^3 a^3}{2\pi^3 D^3\alpha^4}, \quad q_4 = -(q_1+q_2+q_3).$$

Note that in the above expressions for the cumulants of bcc crystals, $\sigma_0^{(1)}, \sigma_0^2, \sigma_0^{(3)}, \sigma_0^{(4)}$ are zero-point energy contributions to the first, second, third and fourth cumulant, respectively, and these cumulant expressions have been obtained for the case of large atomic number N, when the summation over q is replaced by the corresponding integral in the first BZ.

Consequently, all the obtained cumulants contribute to the anharmonic effects described by Eqs. (2) for the anharmonic XAFS of Eq. (1).

3. Numerical Results and Discussions

Now the expressions derived in the previous section are applied to numerical calculations for Fe, a ferrite crystal, using its Morse potential parameters [20] D = 0.4174 eV, α = 1.3885 Å^{-1}. Table 1 shows good agreement of Debye frequency ω_D and temperature θ_D of Fe calculated using the present theory with the experimental values (Expt.) [17] and significant difference from those calculated using the single-bond [5] and single-pair [6] potentials denoted for both by SPP.
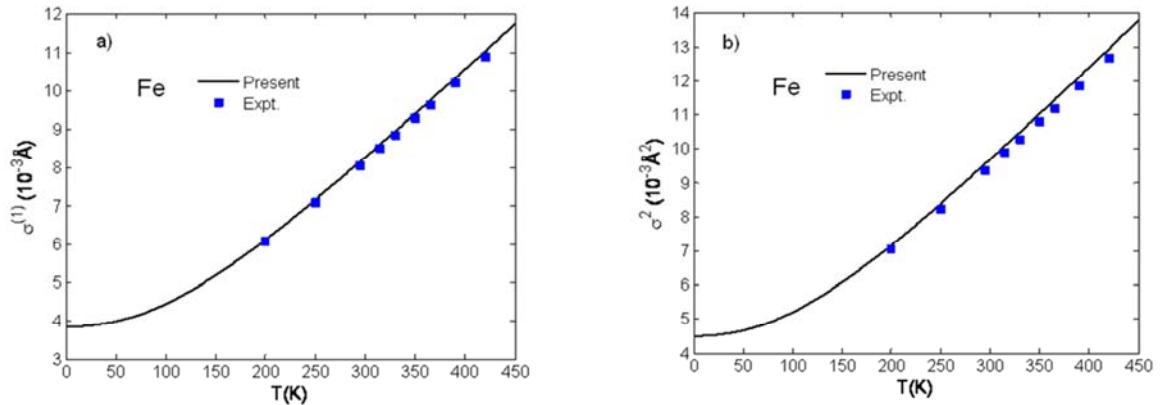
Table 1. Debye frequency ω_D and temperature θ_D of Fe calculated using the present theory compared to the experimental values (Expt.) [17] and to those calculated using the SPP parameters.

| Crystal	ω_D (10^{13}Hz)			θ_D (K)		
	Present	Expt. [17]	SPP	Present	Expt. [17]	SPP
Fe	4.5023	4.5537	3.3252	343.91	358.5±31	253.99
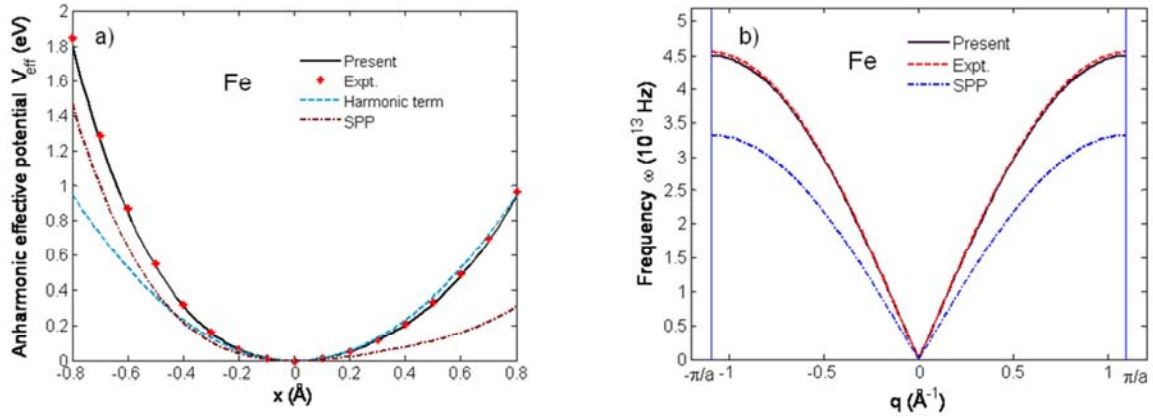
Fig. 1. *a) Anharmonic effective potential and b) dispersion relation of Fe calculated using the present theory compared to experiment [17] and to those calculated using the SPP.*

Figs. 1 illustrate good agreement of the anharmonic effective potential (a) and dispersion relation (b) of Fe calculated using the present theory with experiment [17] where the anharmonic effective potential is asymmetric (compared to the harmonic term) due the anharmonic contributions. They have been used for the calculation and analysis of four first temperature-dependent XAFS cumulants of Fe using the present theory. The good agreement of temperature dependence of the first, second, third and fourth cumulants with the experimental values [17] is presented in Figs. 2a, 2b, 3a and 3b, respectively. Here, at high-temperature the first and second cumulants are linear to the temperature T, the third and fourth cumulants vary as T^2 and T^3, respectively, and at low-temperatures they contain zero-point energy vibration, a quantum effect.

Fig. 2. *Temperature dependence of a) first cumulant $\sigma^{(1)}(T)$ and b) second cumulant $\sigma^2(T)$ of Fe calculated using the present theory compared to the experimental values [17].*
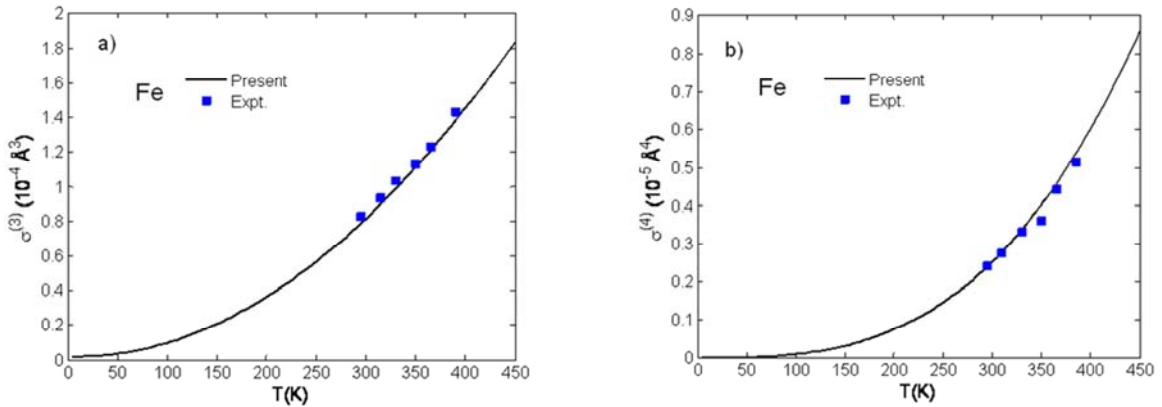
Fig. 3. *Temperature dependence of a) third cumulant $\sigma^{(3)}(T)$ and b) fourth cumulant $\sigma^{(4)}(T)$ of Fe calculated using the present theory compared to the experimental values [17].*

The obtained cumulants have been applied to calculate the anharmonic contributions to XAFS amplitude using the first equation and to XAFS phase using the second equation of Eqs. (2). They contribute to calculating the anharmonic XAFS described by Eq. (1) and then to their Fourier transform magnitudes (FTMs) providing structural information. Fig. 4 shows good agreement of XAFS FTMs for the first shell of Fe at 293 K and 393 K of Fe calculated using Eq. (1) including the anharmonic contributions described by Eqs. (2) containing the above obtained four first temperature-dependent cumulants. These FTMs are shifted when temperature changes from 293 K to 393 K due to the anharmonic effects caused by the temperature dependence.
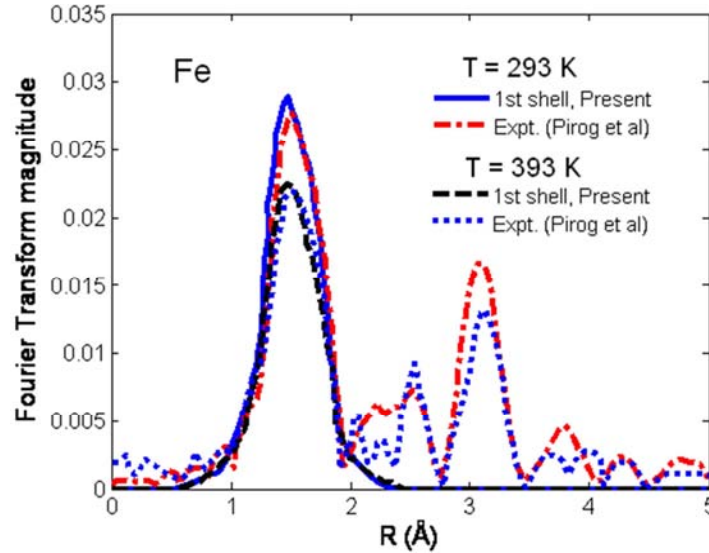

Fig. 4. Fourier transform magnitudes of XAFS for the first shell at 293 K and 393 K of Fe calculated using the present theory compared to experiment [17].

Note that the calculated results of temperature-dependent cumulants of Fe presented in Figs. 2 - 3 and of XAFS FTMs of Fe (Fig. 4) contribute to the valuation of the thermodynamic properties and anharmonic effects in XAFS of Fe. Here, the first cumulant describes the net thermal expansion or disorder, the second one describes the MSRD, the third cumulant or MCRD describes the asymmetry of the pair distribution function, and the fourth one describes the anharmonic contribution to XAFS amplitude. These obtained cumulants describing the high-order expanded DWFs contribute to XAFS spectra and then to their FTMs of bcc crystals, i.e., Fe based on Eqs. (1) and (2). All they provide the accurate information on the thermodynamic properties and structural parameters of bcc crystals, i.e., Fe from XAFS experiment.

4. Conclusions

Thermodynamic properties of bcc crystals have been studied based on their ACDM DWFs expanded up to the fourth order and XAFS FTMs where the ACDM and the anharmonic effective potential have been derived based on the MBPA the FSNNCA, respectively. The obtained results contribute to getting the accurate information on structural and other parameters of bcc crystals taken from XAFS experiment.

The thermodynamic properties of bcc crystals described by the obtained cumulants are characterized by their temperature-dependence, where at high-temperature the first and second cumulants are linear to the temperature T, the

third and fourth cumulants vary as T^2 and T^3, respectively, and at low-temperatures they contain zero-point energy vibration, a quantum effect.

The advantage and efficiency of the present theory in XAFS data analysis are illustrated by the good agreement of the numerical results of four first temperature-dependent cumulants and XAFS FTMs of Fe with experiment. This makes it possible to reproduce the experimental XAFS data of bcc crystals using the present theory.

References

[1] E. D. Crozier, J. J. Rehr, and R. Ingalls, in *X-ray Absorption*, edited by D. C. Koningsberger and R. Prins (Wiley, New York, 1988). Chap. 9.

[2] Tranquada J. M. and R. Ingalls R. (1983). Extended x-ray-absorption fine-structure study of anharmonicity of CuBr. Phys. Rev. B 28, 3520.

[3] Stern A., P. Livins, and Zhe Zhang. (1991). Thermal vibration and melting from a local perspective Phys. Rev. B 43, 8850.

[4] Hung N. V. and Frahm R.. (1995). Temperature and Shell Size Dependence of Anharmonicity in EXAFS. Physica B 208 & 209, 91.

[5] Hung N. V., Tien T. S., Duc N. B., Vuong D. Q. (2014). High-order expanded XAFS Debye-Waller factors of hcp crystals based on classical anharmonic correlated Einstein model. Mod. Phys. Lett. B 28, 1450174.

[6] Frenkel A. I. and Rehr J. J. (1993). Thermal expansion and x-ray-absorption fine-structure cumulants. Phys. Rev. B 48, 585.

[7]   Miyanaga T., Fujikawa T. (1994). Quantum Statistical Approach to Debye-Waller Factor in EXAFS, EELS and ARXPS. III. Application of Debye and Einstein Approximation, J. Phys. Soc. Jpn. 63, 3683.

[8]   Hung N. V. and Rehr J. J. (1997). Anharmonic correlated Einstein model Debye-Waller factors. Phys. Rev. B 56, 43.

[9]   Hung N. V., Duc N. B., Frahm R. R. (2003) A New Anharmonic Factor and EXAFS including Anharmonic Contributions. J. Phys. Soc. Jpn. 72, 1254.

[10] Hung N. V., Tien T. S., Hung L. H., Frahm R. R. (2008). Anharmonic Effective Potential, Local Force Constant and EXAFS of HCP Crystals: Theory and Comparison to Experiment. Int. J. Mod. Phys. B 22, 5155.

[11] Daniel M., Pease D. M., Hung N. V., Budnick J. D. (2004). Local force constants of transition metal dopants in a nickel host: Comparison to Mossbauer studies. Phys. Rev. B 68, 134414.

[12] Hung N. V. and Fornasini P. (2007). Anharmonic Effective Potential, Correlation Effects and EXAFS Cumulants Calculated from a Morse Interaction Potential for fcc Metals. J. Phys. Soc. Jpn. 76, 084601.

[13] Hung N. V., L. H. Hung L. H., Tien T. S., Frahm R. R. (2008). Anharmonic Effective Potential, Local Force Constant and

EXAFS of HCP Crystals: Theory and Comparison to Experiment. Int. J. Mod. Phys. B 22, 5155.

[14] Hung N. V. (2014). Pressure-Dependent Anharmonic Correlated XAFS Debye-Waller Factors. J. Phys. Soc. Jpn. 83, 024802.

[15] Hung N. V., Thang C. S., Toan N. C., Hieu H. K. (2014). Temperature dependence of Debye-Waller factors of semiconductors. VAC. 101, 63.

[16] Hung N. V., Hue T. T., Khoa H. D., Vuong D. Q. (2016). Anharmonic correlated Debye model high-order expanded interatomic effective potential and Debye-Waller factors of bcc crystals. Physica B 503, 174-178.

[17] V. Pirog I. V. and T. I. Nedoseikina T. I. (2003). Study of pair effective potentials in cubic metals. Physica B 334, 123.

[18] Mahan G. D., *Many-Particle Physics* (Plenum, New York, 1990) 2nd ed.

[19] Maradudin A. A., *Dynamical Properties of Solids*, ed. by G. K. Horton and A. A. Maradudin (North Holland, Amsterdam, 1974) Vol. 1, p. 1.

[20] Girifalco L. A. and Weizer W. G. (1959). Application of the Morse Potential Function to Cubic Metals. Phys. Rev. 114, 687.